# The Modelling , Simulation and Control of a 50 kW Vertical Axis Wind Turbine

Bati A. F., Brennan F.

***Abstract*** **This paper presents the modelling, Simulation and control of the APP 50 kW vertical axis wind turbine generating unit which is designed and built by Cranfield University, Department of Offshore, Process & Energy Engineering. Because of the increasing interest of Power Distribution companies to connect medium sized wind turbines to reinforce the Low Carbon future 11 kV networks, unit exploration and investigation will add valuable insight into operation scenarios and their effects on the local network. The main objectives of this work are to model all elements, verify the design figures-, analyse the operational aspects of the drive-train and improve the quality of the generated power with respect to the converter, harmonic filter and controller.**

## I. INTRODUCTION

The integration of wind power into utility systems, especially with LV networks, is an area that is attracting the growing interest of Distribution Network Operators (DNOs) and customers. The development of renewable natural energy has attracted considerable interest in recent years primarily due to concern about environment pollution caused by the burning of fossil fuels , and the continually diminishing reserves of these fuels [1]. The wind turbine generator system provides an environmentally friendly, economical , competitive and socially beneficial means of electricity generation. Much attention has been paid in recent times to the generation of clean energy. These natural and clean sources of energy need to have no by-products associated with their operation [2]. Wind energy is gaining momentum in this field of clean energy due to its relatively low cost. Wind turbines complement the use of other electric power sources by providing a least cost approach under certain conditions. In addition, wind turbines need minimum maintenance. These sizes (25-150 kw units) attract both DNOs and private firms interest with their simplicity , speed to install and energize, and their high reliability and low maintenance.

These smaller turbines can be easily disassembled and moved to a new location and reassembled at new connection point either to an isolated load or to the grid.The most common special feature about wind turbines is the fact that, unlike other generation systems, the power inflow rate is not controllable [3]. In most generation systems, the fuel flow rate, or the amount of energy, applied to the generator controls the output voltage and frequency. The power fluctuates with the variation of winds. The fact that there is no control over the energy source input, the unpredictability of wind and the varying power demands are more than enough concerns to justify the need for a control system, which will regulate the parameters of the wind energy conversion system that needs to be controlled for matched operation of the wind turbine with regard to power supply quality and to comply with grid codes. The following sections detail the 50 kW wind turbine unit components. Their characteristics, simulation models, and control are details so that its reliable operation can be studied.

## II. WIND TURBINE CHARACTERISTICS

The kinetic energy, U of a parcel of air of mass m flowing at upstream speed u in the axial direction (x-direction) of the wind turbine is given by:

$$U = \frac{1}{2}mu^2 = \frac{1}{2}(\rho Ax)u^2 \qquad (1)$$

where, A is the cross–sectional (swept) area of the wind turbine in square metres, ρ is the air density in kg/m$^3$, and x is the thickness of the wind parcel in metres.

The power in the wind $P_w$, is the time derivative of the kinetic energy and is given in (2), which represents the total power available for extraction.

$$P_w = \frac{1}{2}\rho Au^3 \qquad (2)$$

As the wind passes over the turbine, the wind will lose power equal to the power extracted by the turbine. The extracted power is usually expressed in terms of the wind turbine swept area A, because the upstream cross-sectional area is not as physically measurable as the cross-sectional area of the wind turbine.

$$P_{w,ideal} = \frac{1}{2}\rho\left[\frac{8}{9}\left(\frac{2}{3}A_2\right)u_1^3\right] = \frac{16}{27}\left(\frac{1}{2}\rho A_2 u^3\right) \quad (3)$$

The factor 16/27 = 0.59 is called the Betz coefficient. It shows that an actual turbine cannot extract more than 59 per cent of the total power in an undistributed tube of air of the same area (the cross-sectional area equal to the wind turbine swept area).

The fraction of power $P_m$ extracted from the available power in the wind by practical turbines is expressed by the coefficient of performance $C_p$. The actual mechanical power extracted can be written as:

$$P_m = C_p\left(\frac{1}{2}\rho A u^3\right) = C_p P_w \quad (4)$$

The value of $C_p$ is highly non-linear and varies with the wind speed, the rotational speed of the turbine, and the turbine blade parameters such as pitch angle. The variable that combines the effects of the rotational speed and the wind speed is called the tip speed ratio. The tip speed ratio λ, is defined as the ratio between the rectilinear speed of the turbine tip, $\omega_t R$, and the wind speed u as given in (5).

$$\lambda = \frac{\omega_t R}{u} \quad (5)$$

Another variable used to evaluate the wind turbine performance, is the coefficient of torque $C_t$ . The torque coefficient $C_t$, is also a highly non-linear function of tip-speed ratio λ and blade pitch angle β. It is important to recognize the relationship between the power coefficient and the torque coefficient. The torque coefficient $C_t$, is related to the power coefficient $C_p$, through the following relation:

$$C_p(\lambda,\beta) = \lambda C_t(\lambda,\beta) \quad (6)$$

where $P_m$ (W) is the mechanical power, and $C_p$ is the rotor aerodynamic power coefficient - the percentage of the kinetic energy of the incident air mass that is converted to mechanical energy by the rotor - expressed as a function based on the turbine characteristics.

The power coefficient $C_p$ as a function of the tip -speed ratio has a maximum value at which the turbine speed should be controlled in this range in order to give this maximum value. The power coefficient and torque coefficient curves are given by the manufacturer and typical curves are shown in the following figures .

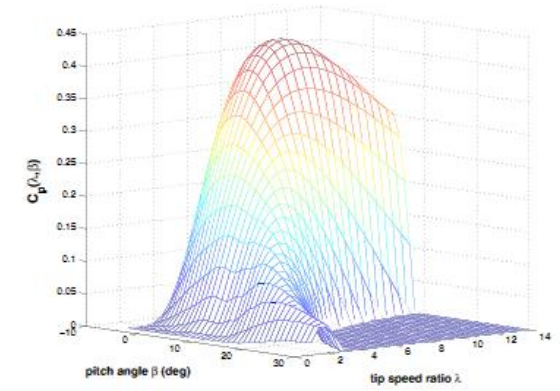


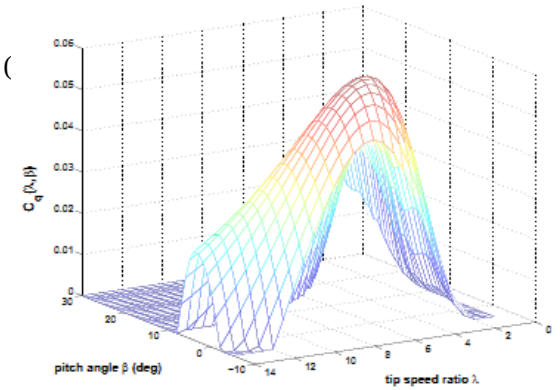


Figure1. Typical Power coefficient and torque coefficient curves.

The rotor mechanical torque $T_m$ is calculated from $P_m$ as:

$$T_m = \frac{P_m}{\omega_t} = f(\omega_t, u, \beta) \quad (7)$$

This expression of the mechanical torque produced by the wind turbine has nonlinearity, being a function of the second power of wind speed, and may be linearized by expanding it as a Taylor series around an operating point with respect values $\omega_{to}, u_o \text{ and } \beta_o$ .

$$T_m = f(\omega_{to}, u_o, \beta_o) + \frac{\partial f}{\partial \omega_t}\Delta\omega_t + \frac{\partial f}{\partial u}\Delta u + \frac{\partial f}{\partial \beta}\Delta\beta + . \quad (8)$$

where partial differentials are computed around the operating point, and the delta terms represent the change in the variables. Neglecting higher order terms, we can write:

$$\Delta T_m = \gamma \Delta\omega_t + \alpha \Delta u + \delta \Delta\beta \quad (9)$$

where $\gamma = \frac{\partial T_m}{\partial \omega_t}$ , $\alpha = \frac{\partial T_m}{\partial u}$ , $\delta = \frac{\partial T_m}{\partial \beta}$ at the operating point . (10)

The parameters $\gamma$, α and δ represent the wind turbine dynamics which are partial derivatives of the aerodynamic torque with respect to the angular turbine speed, the wind speed and pitch angle respectively. They are the rates of change of aerodynamic torque with turbine angular speed, wind speed and pitch angle, respectively, at the operating point about which the system is linearized. These linearization constants (gains) are essentially a steady state representation of the rather complex aerodynamics of the rotor and as such have a considerable uncertainty with which the control system must cope. $\gamma$, α and δ change rapidly, by an order of magnitude or more as the wind speed varies. These gains can be calculated using the following[4]:

$$\alpha = \frac{\partial T}{\partial u} = \frac{1}{2}\rho A R u_{OP}\left[2C_t|_{OP} - \lambda|_{OP}\frac{\partial C_t}{\partial \lambda}|_{OP}\right]$$

$$\delta = \frac{\partial T}{\partial \beta} = \frac{1}{2}\rho A R u^2\left[\frac{\partial C_t}{\partial \beta}\right]_{OP}$$

$$\gamma = \frac{\partial T}{\partial \omega} = \frac{1}{2}\rho AR[\frac{\partial C_t}{\partial \omega}]u^2 \quad (11)$$

To obtain the steady-state solution of the aerodynamic forces and torques acting on the blade of the turbine, a numerical method may be used for this purpose.

We can deduce a similar equation for thrust which is perpendicular to the torque and write:

$$\begin{bmatrix}\Delta T_m \\ \Delta T_r\end{bmatrix} = \begin{bmatrix}\gamma & \alpha & \beta \\ \gamma' & \alpha' & \beta'\end{bmatrix}\begin{bmatrix}\Delta\omega_t \\ \Delta u \\ \Delta\beta\end{bmatrix} \quad (12)$$

where J= $\begin{bmatrix}\gamma & \alpha & \beta \\ \gamma' & \alpha' & \beta'\end{bmatrix}$ is the Jacobian matrix which contains the aerodynamic gains at the operating point o.

Now, the change in the three variables namely $\omega_t, u, \beta$ can be obtained by solving the following:

$$\begin{bmatrix}\Delta\omega_t \\ \Delta u \\ \Delta\beta\end{bmatrix} = J^{-1}.\begin{bmatrix}\Delta T_m \\ \Delta T_r\end{bmatrix} \quad (13)$$

We start the solution with estimated values of the three variables to calculate the change in torque and thrust. Then, we add these changes in the three variables to the initial values and repeat the process until the corrections become so small that they satisfy a chosen precision index.

For example, for the first step:

$$T_m = T_{mo} + \Delta T_m^{(o)} \quad (14)$$

And similarly, we can update the thrust value for each step of the solution, depending on the new calculated values of the three variables, such as ,for example:

$$\omega_t = \omega_{to} + \Delta\omega_t^{(o)} \quad (15)$$

Finally, the solution stops when we attain a specified precision index.

Applying Laplace Transforms to equation 9 yields:

$$\Delta T_m(S) = \gamma \Delta\omega_t(S) + \alpha \Delta u(S) + \delta \Delta\beta(S) \quad (16)$$

This is a linear equation describing the wind turbine dynamics in the Laplace domain (S-domain).

A block diagram of the linear turbine is depicted in Figure 2.

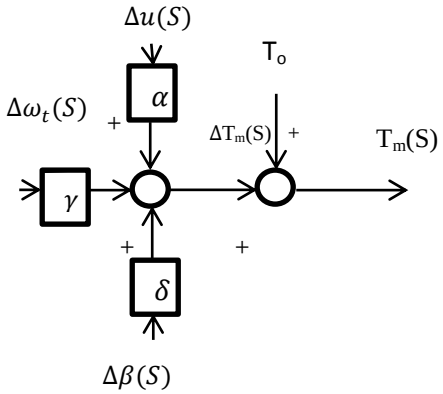


Figure2. Turbine Block Diagram

The wind turbine mechanical power $P_m$ , is equal to the product of the aerodynamic torque $T_m$ , and the rotational speed $\omega_t$ .

$$P_m = T_m . \omega_t \quad (17)$$

The aerodynamic torque $T_m$ that turns the rotor shaft is related to the torque coefficient $C_t$ , and is represented by equation 18:

$$T_m = \frac{1}{2}\rho A R C_t(\lambda, \beta)u^2 \quad (18)$$

where, ρ is the air density, A is the swept area of the wind turbine, R is the maximum radius of the wind turbine, u is the upstream wind speed , and $C_t$ is the torque coefficient.

As is obvious from the equation which represents the change in the torque equ.9 and equation 18, the torque of a specific turbine, is a function of wind speed, turbine angular velocity and pitch angle for fixed air density.

## III. DRIVE TRAIN

The drive-train converts the input aerodynamic torque on the rotor into the torque on the low-speed shaft which is scaled down through the gearbox and then induces a torque on the high-speed shaft. Figure 3 illustrates a schematic diagram for the drive-train transmission system[5].

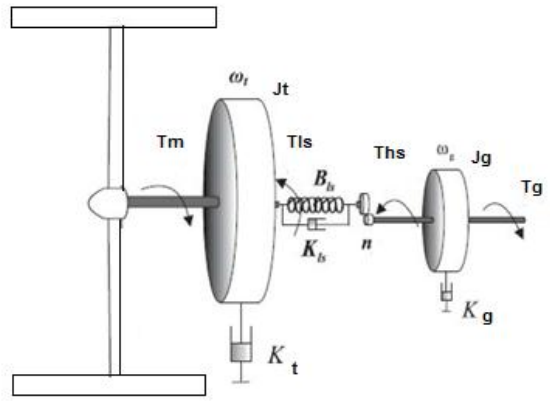


Figure 3. Two-mass wind turbine system

The rotor-side inertia $J_t$ dynamics is given by:

$$J_t \frac{d\omega_t}{dt} = T_m - T_{ls} - K_t\omega_t \quad (19)$$

The low-speed shaft torque $T_{ls}$ is:

$$T_{ls} = B_{ls}(\theta_t - \theta_{ls}) + K_{ls}(\omega_t - \omega_{ls}) \quad (20)$$

The generator inertia $J_g$ is driven by the high-speed shaft and braked by the electromagnetic torque $T_g$ of the generator:

$$J_g \frac{d\omega_g}{dt} = T_{hs} - K_g\omega_g - T_g \quad (21)$$

The gear ratio is:

$$n=\frac{T_{ls}}{T_{hs}}=\frac{\omega_g}{\omega_t}=\frac{\theta_g}{\theta_{ls}} \quad (22)$$

where $J_t$ is the turbine rotor moment of inertia in kg-m$^2$

$\omega_t$ is the low-speed shaft angular speed in rad/sec$^2$

$\omega_g$ is the high-speed shaft angular speed in rad/sec$^2$

$K_t$ is the turbine damping coefficient in N.m/rad/sec (representing the aerodynamic resistance taking place in the blade)

$Kg$ is the generator damping coefficient in N.m/rad/sec(which corresponds to mechanical friction and windage)

$K_{ls}$ is the low-speed shaft damping coefficient in N.m/rad/sec

$T_m$ is the turbine torque in N.m

$T_{ls}$ is the low-speed shaft torque in N.m

$J_g$ is the generator rotor moment of inertia in kg-m$^2$

$T_{hs}$ is the high-speed shaft torque in N.m

Taking the time derivative of equation 20 and using equations 19 and 21, we get the following, which will be used in the Simulink model:

$$\frac{dT_{ls}}{dt} = \left(B_{ls} - \frac{K_{ls}K_t}{J_t}\right)\omega_t + \frac{1}{n}\left(\frac{K_{ls}K_t}{J_g} - B_{ls}\right)\omega_g - K_{ls}\left(\frac{J_t+n^2J_g}{n^2J_tJ_g}\right)T_{ls} + \frac{K_{ls}}{J_t}T_\alpha + \frac{K_{ls}}{nJ_g}T_g$$

where $K_{ls}$=I.G/$L_{ls}$

$D_{ls}=\xi D_s$

$$\xi = \sqrt{1-(\frac{\omega}{\omega_n})^2}$$

$$D_s=2\sqrt{K_{ls}m} \quad (23)$$

$\frac{\omega}{\omega_n}$ = ratio of shaft frequency of oscillation to the undamped natural frequency of the shaft.

$m$=mass of the shaft

I= second momentum of area about the axis of rotation

$L_{ls}$=shaft length

G= modulus of rigidity for shaft material

$D_s$= critical damping of shaft

$\xi$= damping ratio of the shaft [6]

The state-space dynamical model of the transmission system is as follows:

$$\begin{bmatrix} \dot{\omega}_t \\ \dot{\omega}_g \\ \dot{T}_{ls} \end{bmatrix} = \begin{bmatrix} a_{11} & a_{12} & a_{13} \\ a_{21} & a_{22} & a_{23} \\ a_{31} & a_{32} & a_{33} \end{bmatrix} \begin{bmatrix} \omega_t \\ \omega_g \\ T_{ls} \end{bmatrix} + \begin{bmatrix} b_{11} \\ b_{21} \\ b_{31} \end{bmatrix} T_m + \begin{bmatrix} b_{12} \\ b_{22} \\ b_{32} \end{bmatrix} T_g \quad (24)$$

where the a's and b's coefficients are derived from system parameters defined above.

## IV. GENERATOR-CONVERTER

PMSG: The power train is composed of Permanent Magnet Synchronous Generator and Power Electronics Converter capable of driving the PMSG in motor and regenerative modes. Figure 4 shows the generator –converter with the turbine.

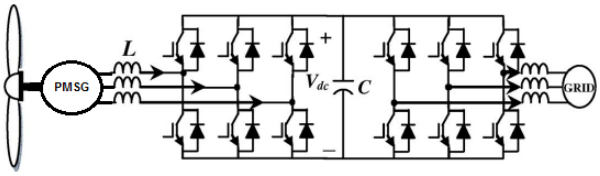


Figure 4. The PMSG –Converter-Grid System

The mathematical model of the PMSG is as follows[7]:

$$v_q = -\left(r + \frac{d}{dt}L_q\right)i_q - \omega_r L_d i_d + \omega_r \lambda_{PM}$$

$$v_d = -\left(r + \frac{d}{dt}L_d\right)i_d + \omega_r L_q i_q$$

$$T_e = \frac{3}{2}\left(\frac{P}{2}\right)\left[(L_d - L_q)i_q i_d - \lambda_{PM} i_q\right]$$

$$J_g \frac{d\omega_r}{dt} = T_g - T_d - T_e \qquad (25)$$

where $T_d$ is the generator damping torque which is generated from the mechanical friction and windage effects of the generator rotor ,and from electrical damping . The electrical damping is due to the action of damper winding in the rotor and the AC winding on the stator.

The above voltage equations and the electromagnetic torque are for the PMSG in the dq-axis synchronous rotational reference frame, where $vq$ , $Iq$ , $Lq$ are the q-axis voltage, current and inductance, $v_d, i_d, L_d$ are the corresponding d-axis quantities, r is the phase resistance, $\omega_r$ ,is the generator angular speed and $\lambda_{PM}$is the flux linkage produced by the permanent magnets, and where the angular generator speed $\omega_r$ can be expressed in terms of the angular rotor mechanical speed $\omega_g$ as:

$$\omega_r = \frac{p}{2}\,\omega_g$$

Where p is the number of magnetic poles of the generator.

RECTIFIER: The converter composed of rectifier and inverter connected through a DC link with shunt capacitance to smooth the DC voltage ripple. The rectifier function is to convert the AC power output of the PMSG into DC power.

Fig. 5 shows a typical three-phase, 6-pulse diode rectifier circuit, in which $L$ and $r$ represent the combined effect of the cable and inductor leakage inductances and resistances, respectively. $L_{dc}$ and $r_{dc}$ are the inductance and resistance of the dc-link inductor, respectively and $U_{dc}$ is the voltage across the dc-link capacitor $C$. It is assumed that the AC voltages of the PMSG are balanced, sinusoidal and given by[8]:

$$V_{Sa} = V_m \sin(\omega_s t + \frac{\pi}{2})$$
$$V_{Sb} = V_m \sin(\omega_s t - \frac{\pi}{6})$$
$$V_{Sc} = V_m \sin(\omega_s t - \frac{5\pi}{6}) \qquad (26)$$

where $V_m$ is the peak phase voltage and $\omega_s$ denotes the angular frequency of the AC output of the PMSG. An important feature of the diode rectifier is the current-commutation, as shown in Fig. 6, during which two diodes in the same groups (D1, D3, D5) or (D2, D4, D6) may conduct due to the presence of the input inductance $L$. The ccommutation interval increases with the load current. For the 6 pulse diode rectifier, the current-commutation and conduction intervals repeat in every 60 electrical degrees.

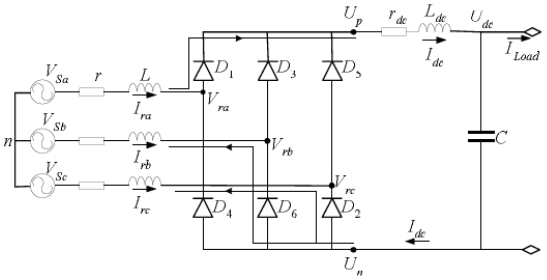


Figure 5. 6-pulse diode rectifier

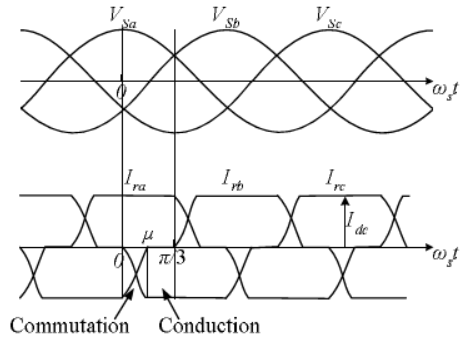


Figure 6. AC Voltage and Current waveforms

The averaged-value model of a 6-pulse rectifier is :

$$\frac{dI_{DC}}{dt} = g_1(I_{DC}, \mu) + g_2(V_m, \mu) + g_3(U_{DC}, \mu) \qquad (27)$$

where

$$g_1 = -\frac{3}{\pi}\left[\frac{R_{D1}}{L_{D1}} - \frac{R_{D2}}{L_{D2}}\right]\mu I_{DC} - \frac{R_{D2}}{L_{D2}} I_{DC}$$

$$g_2 = \frac{3}{\pi} V_m \left[\frac{3}{2L_{D1}}\sin\mu - \frac{\sqrt{3}}{L_{D2}}\sin\left(\mu - \frac{\pi}{6}\right) + \frac{1}{L_{D2}}\frac{\sqrt{3}}{2}\right]$$

$$g_3 = -\frac{3}{\pi}\left(\frac{1}{L_{D1}} - \frac{1}{L_{D2}}\right)\mu U_{DC} - \frac{1}{L_{D2}} U_{DC} \qquad (28)$$

Assuming that the commutation angle $\mu$ is kept unchanged over a diode switching period $T=\pi/3\omega s$, the average value of the DC-link voltage and current over the $T$ period can be obtained by using the state-space averaging technique described by Liqiu Han[8]. The resulting dynamic equation for

the DC-link current is given in (27). When the resistance $r$ is neglected, $\mu$ is given by

$$\mu = \cos^{-1}\left(1 - \frac{2\omega_s L}{\sqrt{3}V_m} I_{DC}\right) \quad (29)$$

Since $\mu$ is now only dependant on $I_{DC}$ ,equation (27) is non-linear but time-invariant.

INVERTER: The function of the inverter is to invert the DC power output of the rectifier into AC power with fixed frequency as the grid frequency. The inverter has six IGBTs to perform power inversion using the PWM technique with power and current control loops. The inverter connected to the grid through the LC filter is shown in Fig. 7 below.

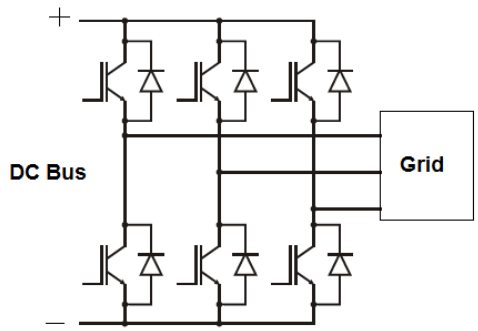


Figure 7. 6-pulse IGBT inverter

The inverter model includes phase-locking functions , internal control loops an outer power regulation loop, a measurement of average power and a phase-locked loop[9]. This model is shown in Fig. 8 below.

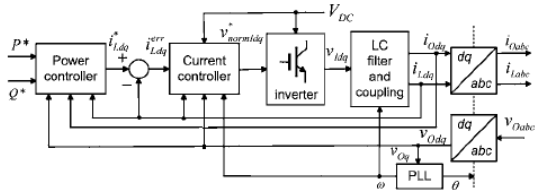


Figure 8. Voltage Source Inverter with power and current control.

The state-space model of the inverter is :

$$\dot{\boldsymbol{x}} = \boldsymbol{A}\boldsymbol{x} + \boldsymbol{R}(\boldsymbol{x}, \boldsymbol{u})$$
$$\boldsymbol{y} = \boldsymbol{S}(\boldsymbol{x}, \boldsymbol{u}) \quad (30)$$

where $x$ represents state variables of the inverter system and can be detailed in the following figure.

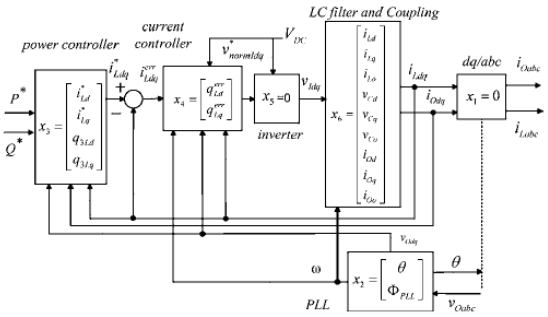


Figure 9. Topology of the inverter with each sub-system states.

$R$ represents input vector which is a function of some of the states and driving inputs u. Where u is

$$\boldsymbol{u}_{\mathrm{CCI}} = \left[\, V_{\mathrm{DC}} \quad v_{\mathrm{Oa}} \quad v_{\mathrm{Ob}} \quad v_{\mathrm{Oc}} \quad P^* \quad Q^* \,\right]^{\mathrm{T}} \quad (31)$$

And $y$ is the output vector that represents filter currents and output current flowing into the grid as shown in figure 8 .

## V. SIMULATION RESULTS

ROTOR: A Simulink model is used to simulate the performance of the rotor. This model is shown in Fig. 10 below:

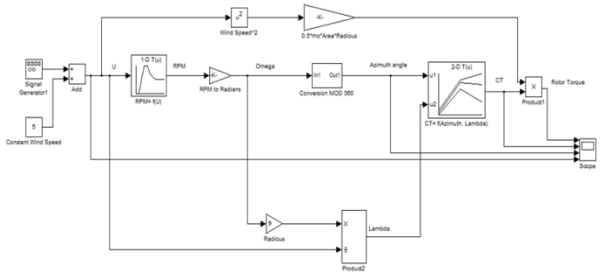

Figure 10. Rotor Simulink Model

where the input is the wind speed as a constant and some added distortion to represent the actual turbulence variations and the output is the mechanical torque of the rotor. Some of the results are shown in Figs. 11 and 12.

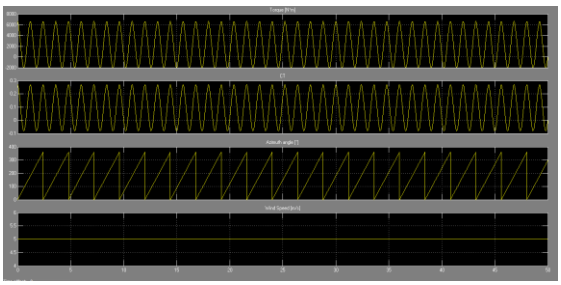

Figure 11. Torque, torque coefficient, azimuth angle and wind speed for 5 m/s without distortion.

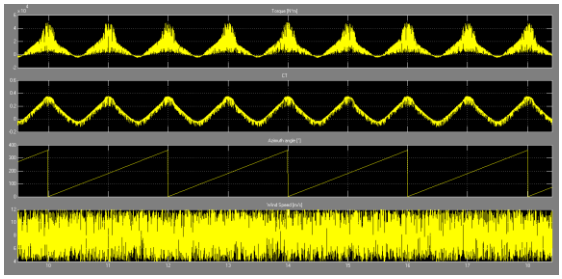

Figure 12. Torque, torque coefficient, azimuth angle and wind speed for 8 m/s with distortion.

MECHANICAL TRANSMISSION SYSTEM: This is composed of torque tube ,ball bearings, flexible couplings and gear box. The model uses lumped moment of inertia, stiffness and damping coefficients. The Simulink model is shown in Fig. 13 below:

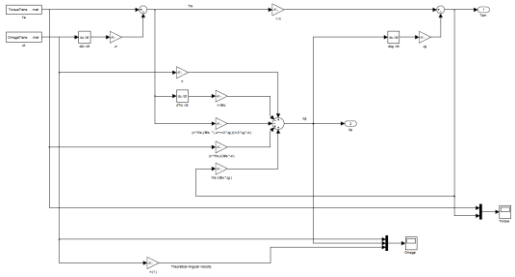

Figure 13. Simulink model of Transmission System

The inputs are the mechanical torque produced by the rotor and the angular rotor speed of the low-speed shaft. The outputs are the torque and angular speed of the high-speed shaft.
The simulation results are shown in Fig.s 14 and 15 below, and the effect of torque ripple on the angular speed of the generator is obvious:

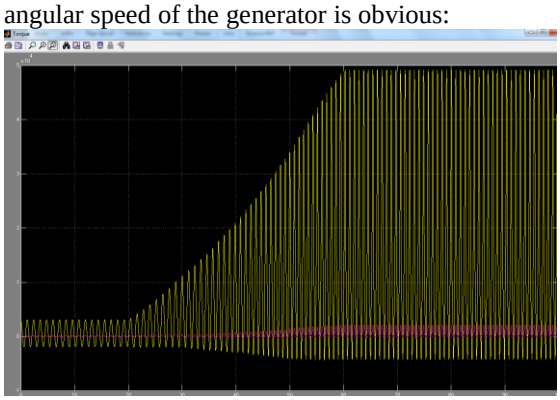

Figure 14. Low- and High-speed shafts Torques

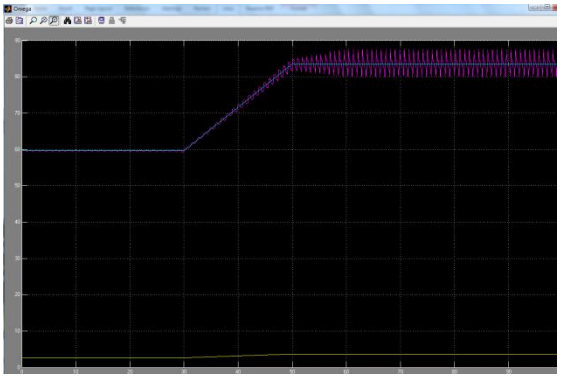

Figure 15 Low-& High-speed shaft angular speeds

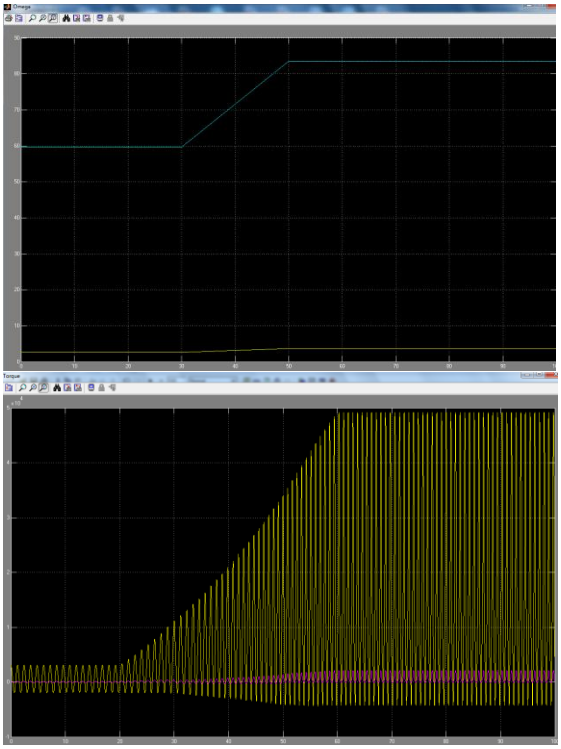

Figure 16 Speed and torque with increased damping

As shown in Fig. 16 the angular speed of generator shaft is almost free from ripple caused by the rotor of the turbine. This result can be obtained from a well-designed transmission system. Also, an artificial damping can be added if there is a pitch angle control accessibility to the turbine blades in case there are limitations to design optimum transmission body.

GENERATOR-CONVERTER: The electrical parts of the unit are the PMSG, converter , PI Controller and filter.
The operating points of the machine are extracted from the motor and generator modes at steady state assuming only active power being used by the machine. The following phasor diagrams are used in the analysis.

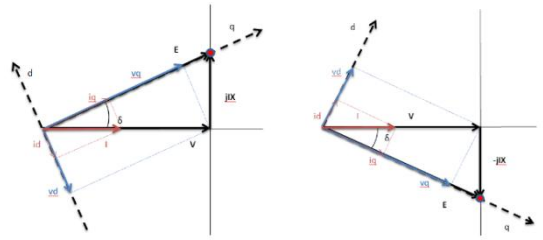

Figure 17. Generator and motor operation phasor diagrams.

The Simulink Model is shown in Fig.16 below:

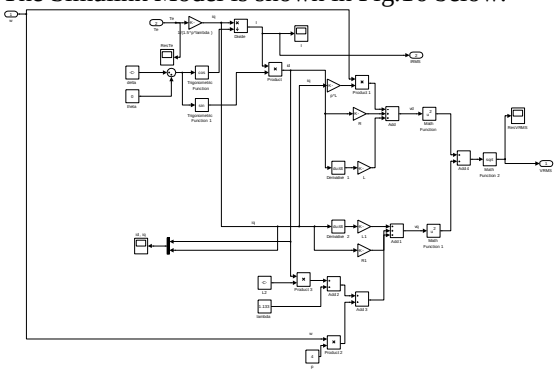

Figure 18. PMSG Simulink Model

The voltage and current wave forms for inductive load are shown in Fig. 19 below. As it is clear that the LC filter at the output of the inverter has a significant impact on harmonics removal from voltage wave form.

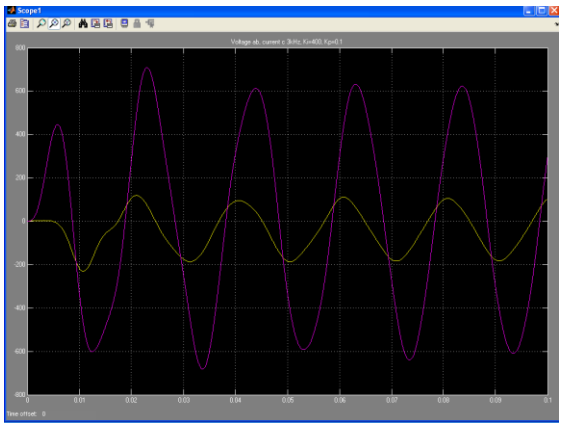

Figure 19. Output voltage and current wave forms of an inductive load.

The voltage wave form at the terminals of the inverter and before it is going to be filtered by the LC filter is shown in Fig. 20 below:

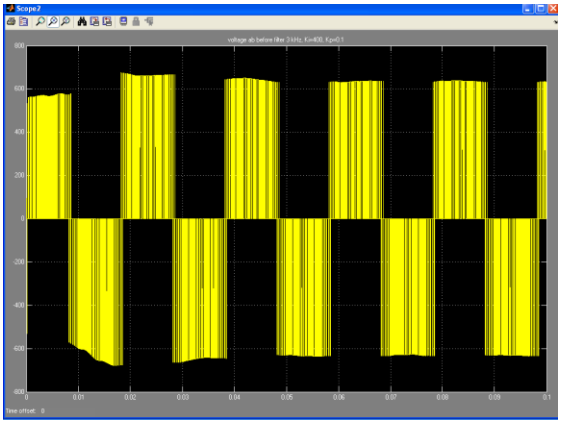

Figure 20. The voltage wave form of the inverter output.

The DC voltage output of the rectifier is shown in Fig. 21 below:

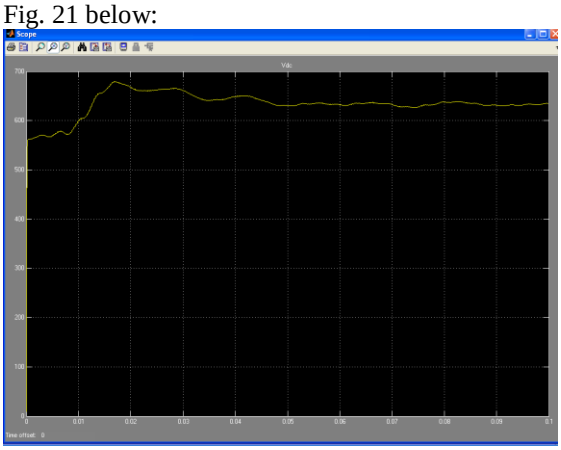

Figure 21. The DC voltage of the DC link

The linearized model of the whole unit with the PI controller is shown in Fig. 21 below:

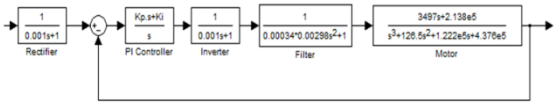


Figure 22. The linearized model of the unit with PI current controller.

The linearized model can be obtained either from Simulink or from a reduced-order model of the system state-space[10].

The root locus and time domain of the controlled system is shown in Fig.23 below:

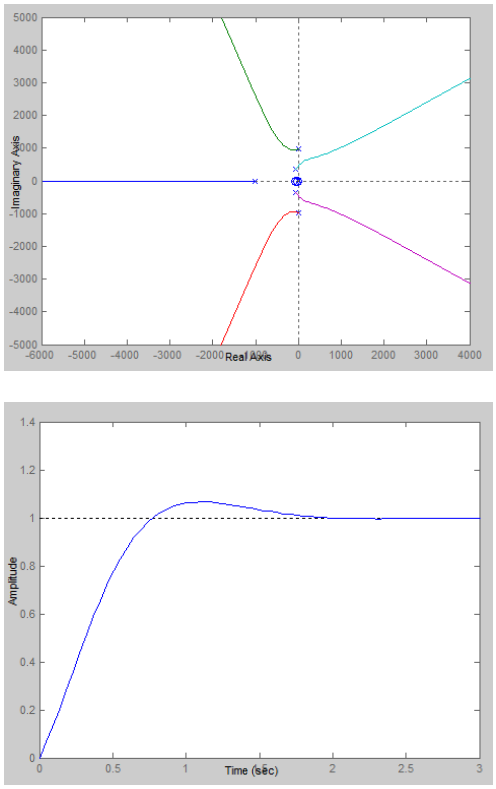


Figure 23. Root locus and system step response.

## VI. CONCLUSIONS

In this work the exploration, analysis ,simulation and operation control are carried out for a 50 kW vertical-axis wind turbine.

Some of the simulation results were compared with the experimental data obtained from Unidrive interfacing and data acquisition unit installed in the test site of the wind turbine. A good degree of agreement found between the two sets of data.

The tests showed that the voltage, current and power controllers achieved the required operational specifications.

The most important feature of this type of wind turbines is the torque ripple created by the nature of the rotor and the aerodynamic interaction with turbine blade.

This problem is neutralised by the action of the converter and its controllers so that the output power is levelled and has minimum ripple effects.

It was suggested throughout this paper that by proper design of transmission system(low-speed shaft, gear box, and high-speed shaft), the ripple can be minimized to a low level.

If the new designed transmission system is not acceptable in terms of masses ,stiffness and damping then we suggest to introduce dynamic electromagnetic brake that will operate in such a manner to cancel torque ripple and can be used for emergency brake as well.

## VII. REFERENCES


1. Xing-Fang Z., Da-Ping X., and L. Bing Yi., “Adaptive Optimal Fuzzy Control For Variable Speed Fixed Pitch Wind Turbines”, IEEE Proc. of the 5th World Congress on Intelligent Control and Automation, 15-17 June 2004, Hang Zhou, P.R. China.
2. Moor G. D. and Beukes H. J., “Maximum Power Point Trackers For Wind Turbines”, The 35th IEEE Power Electronics Specialists Conference, 2004, Aachen, Germany.
3. Chedid R., F. Mrad, and M. Basma, “Intelligent Control of a Class of Wind Energy Conversion System”, IEEE Trans. Energy Conversion, Vol.14, No.4, pp.1597-1604, December 1999.
4. Bati A. F., Leiab S. “ NN self-Tuning pitch angle controller of wind power Generation Unit”, 2006 IEEE power systems conference, 29-30 Oct.2006, Atlanta GA USA, pp.2019-2029 ,
5. Boukhezzar B., Siguerdidjane S. ,” Comparison Between Linear and Nonlinear Control Strategies for Variable Speed Wind Turbine Power Capture Optimization “ EVER 2009, Monaco, France, , 26 March 2009.
6. C. F Beards, “ Structural Vibration: Analysis and Damping” ISBN 0470235861 (0-470-23586-1)
7. Chee-Mun Ong, “ Dynamic Simulation of Electrical Machinery: Using MATLAB/SIMULINK”, Prentice Hall PTR | ISBN / ASIN: 0137237855.
8. Liqiu Han, Jiabin Wang and David Howe,” State-space average modelling of 6- and 12-pulse diode rectifiers” Proc. Of 12th European Conference on Power Electronics and Applications (EPE) 2007, Aalborg, Denmark, Paper ID 639. 2007.
9. N. Kroutikova, C.A. Hernandez-Aramburo and T.C. Green ,” State-space model of grid-connected inverters under current control mode”, IET Electric Power Applications, Vol. 1, No. 3, pp. 329-33, 2007.
10. Bati A. F. " Reduced-order model for power system transient stability studies" Engineering and Technology journal, pp(341-349),Vol.17, No.4, 1998.

Appendix
PMSG :LSLEROYSOMER, Frame
GLSRPM315MR
PMSG voltage 400 V.
Frequency 50 Hz
Phase resistance 0.06 ohm
Phase inductance 1.89 mH
PMSG power rating 110 kW
Speed 750 rpm
Number of poles 8
Full load Torque 1401 Nm
LC Filter: R 0.056 ohm
C 50 Mf
L 1.35 mH
Voltage and current PI controller: $K_p$=1, $K_I$=400
Storage batteries: LifBatt 86 kWh ,780 V. DC
Unidrive SPM 400 V.: Emerson , Control Techniques
Rotor: Two blade H-Type
Mean torque 13 kNm
Peak torque 50 kNm
Rated rotational speed 35 rpm
Gear Box: SEWEURODRIVE
Input speed 750 rpm
Input power 55 kW
Ambient Temperature 0-30$^{o}$C
Nominal Power 188 kW
Nominal output torque 52.1 kNm
Gear ratio 22.78
Service factor 3.4